APPENDIX

A.1 Determination of the lowest-energy structures of Ni_{n+1} clusters

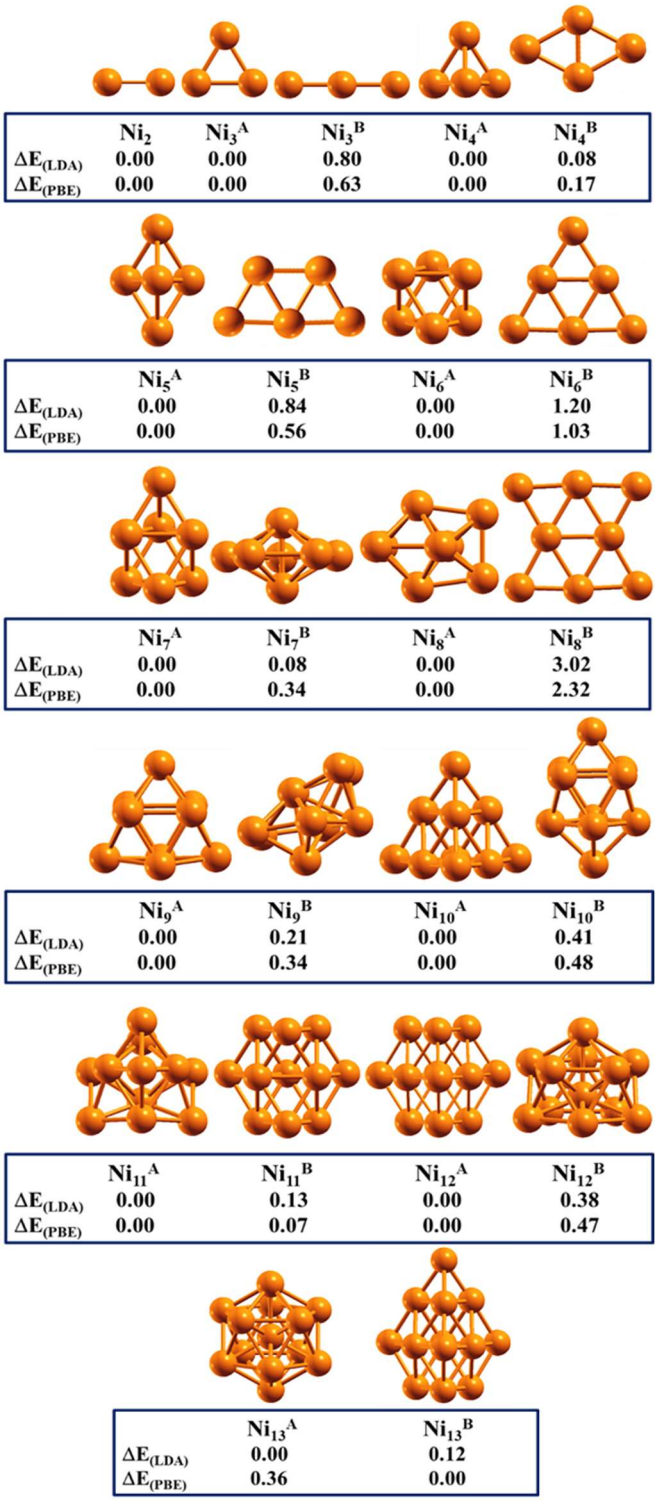

Figure A.1: Structures of Ni_{n+1} clusters ($1 \leq n \leq 12$) with relative energy difference (ΔE) obtained with LDA and PBE functionals. The zero value of ΔE display the ground-state structure of Ni_{n+1} clusters.

A.2 Determination of the lowest-energy structures of Ni $_n$Cu clusters

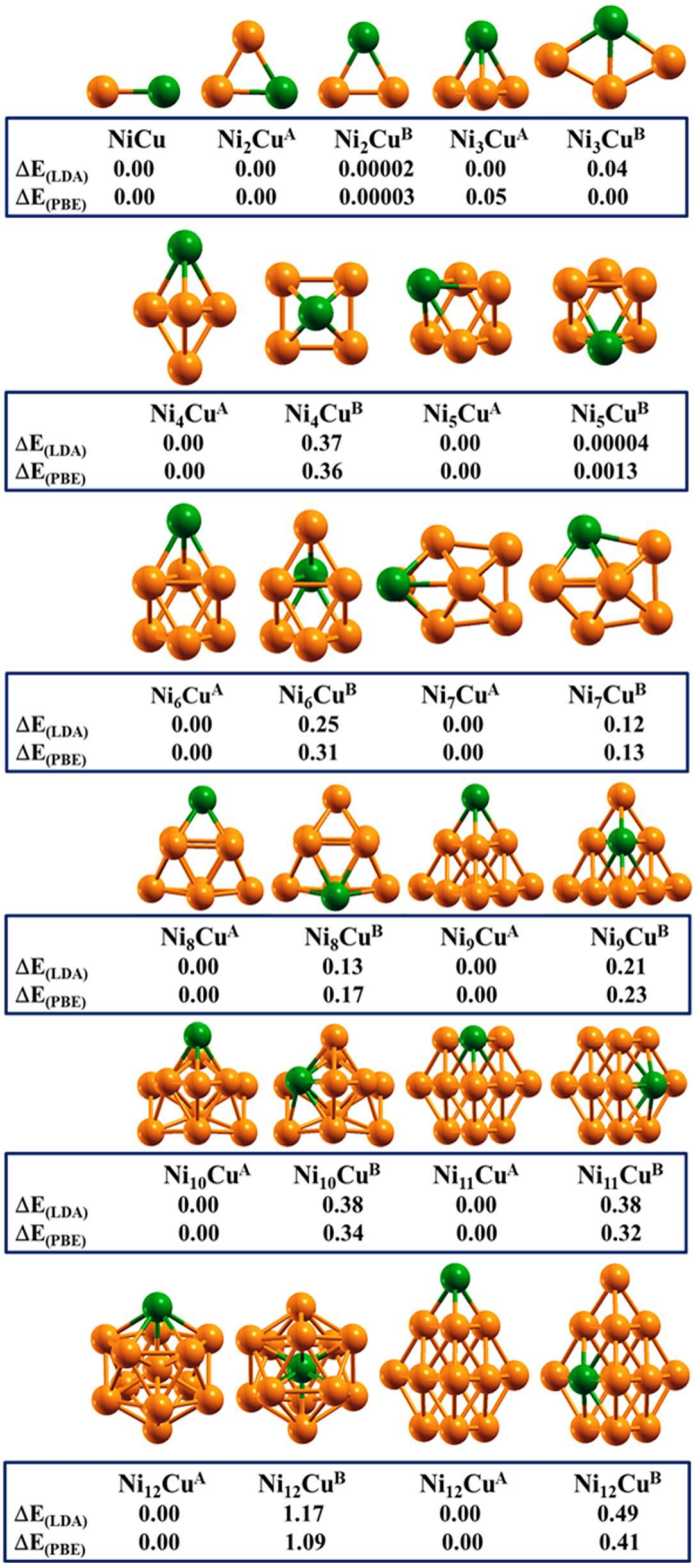

Figure A.2: Structures of Ni_nCu clusters ($1 \leq n \leq 12$) with relative energy difference (ΔE) obtained with LDA and PBE functionals. The zero value of ΔE display the ground-state structure of Ni_nCu clusters.

A.3 Determination of point-group symmetry (structure) of Ni_{n+1} and Ni_nCu clusters ($1 \leq n \leq 12$)

Table A.1: The point-group symmetry (structure) of Ni_{n+1} and Ni_nCu clusters ($1 \leq n \leq 12$).

Cluster	Symmetry (Structure)	Cluster	Symmetry (Structure)
	LDA		LDA
Ni_2	$D_{\infty h}$ (Dimer)	NiCu	$C_{\infty v}$ (Linear)
Ni_3	C_s (Equilateral triangle)	Ni_2Cu	C_s (Isosceles triangle)
Ni_4	C_1 (Tetrahedron)	Ni_3Cu	C_{3v} (Tetrahedron)
Ni_5	D_{3h} (Trigonal bipyramid)	Ni_4Cu	C_{3v} (Distorted trigonal bipyramid)
Ni_6	C_i (Octahedron)	Ni_5Cu	C_{4v} (Distorted Octahedron)
Ni_7	C_{3v} (Capped octahedron)	Ni_6Cu	C_{3v} (Capped octahedron)
Ni_8	D_{2d} (Bicapped octahedron)	Ni_7Cu	C_s (Bicapped octahedron)
Ni_9	C_{3v} (Tricapped Trigonal Prism)	Ni_8Cu	C_s (Tricapped Trigonal Prism)
Ni_{10}	T_d (Tetracapped square bipyramid)	Ni_9Cu	C_3 (Tetracapped square bipyramid)
Ni_{11}	C_{3h} (Tetracapped pentagonal Bipyramid)	$Ni_{10}Cu$	C_s (Tetracapped pentagonal Bipyramid)
Ni_{12}	C_{3h} (Anticuboctahedron)	$Ni_{11}Cu$	C_s (Anticuboctahedron)
Ni_{13}	I_h (Icosahedron)	$Ni_{12}Cu$	C_{5v} (Icosahedron)

A.4 Determination of structural stability and relative energetics

To investigate the influence of the doped Cu atom on the stabilities of Ni clusters, we concentrate our focus on the relative stabilities of Ni and Cu doped Ni clusters. The most stable structures are analysed through average bond length (d_{av}) (see Eqn. 3.2), averaged binding energy per atom (E_b), second-order difference of energies ($\Delta^2 E$), and fragmentation energies (ΔE_F), by using the following formulas,

$$E_b(Ni_{n+1}) = \frac{[(n+1) \times E(Ni) - E(Ni_{n+1})]}{(n+1)} \quad (A.1)$$

$$E_b(Ni_nCu) = \frac{[n \times E(Ni) + E(Cu) - E(Ni_nCu)]}{(n+1)} \quad (A.2)$$

$$\Delta^2 E(Ni_{n+1}) = E(Ni_{n+2}) + E(Ni_n) - 2E(Ni_{n+1}) \quad (A.3)$$

$$\Delta^2 E(Ni_nCu) = E(Ni_{n+1}Cu) + E(Ni_{n-1}Cu) - 2E(Ni_nCu) \quad (A.4)$$

$$\Delta E_F(Ni_{n+1}) = E(Ni_n) + E(Ni) - E(Ni_{n+1}) \quad (A.5)$$

$$\Delta E_{F(Cu)}(Ni_nCu) = E(Ni_n) + E(Cu) - E(Ni_nCu) \quad (A.6)$$

$$\Delta E_{F(Ni)}(Ni_nCu) = E(Ni_{n-1}Cu) + E(Ni) - E(Ni_nCu) \quad (A.7)$$

Where, $E(Ni_{n+1})$, $E(Ni_nCu)$, $E(Ni_{n+2})$, $E(Ni_{n+1}Cu)$, $E(Ni_{n-1}Cu)$, and $E(Ni_n)$ represent the total energies of the lowest-energy structures of Ni_{n+1}, Ni_nCu, Ni_{n+2}, $Ni_{n+1}Cu$, $Ni_{n-1}Cu$ and Ni_n clusters respectively. The $E(Ni)$ and $E(Cu)$ represent the atomic energy of isolated Pd and Cu atoms, respectively. n represents the number of atoms. The computed E_b, $\Delta^2 E$ and ΔE_F along with total magnetic moment (M_T) and magnetic moment per atom ($M_{\mu B}$/atom) for Ni_{n+1} and Ni_nCu clusters with LDA and PBE functionals are summarized in Figure A.3(a-f) and Figure A.3(g-l) respectively. The experimental values of total magnetic moment and magnetic moment per atom of Ni_{n+1} clusters are also included in the Figure A.3(f-g) for the sake of comparison (*Phys. Rev. Lett.* **1996**, *76*, 1441).

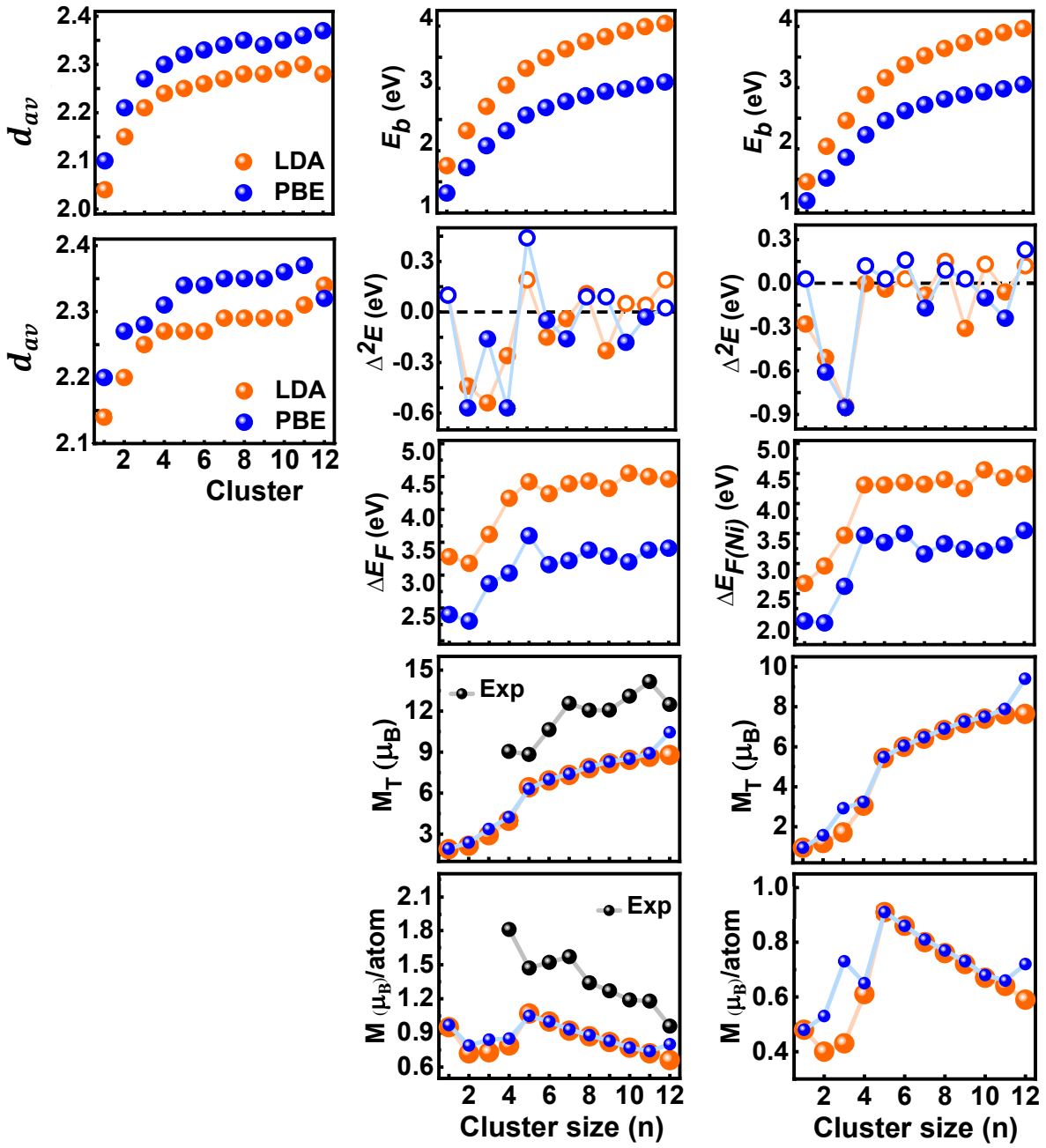

Figure A.3: The average bond length (d_{av}) of (a) Ni_{n+1} and (b) Ni_nCu clusters (1 ≤ n ≤ 12). The averaged binding energy per atom (E_b), second-order energy difference (Δ^2E), fragmentation energy (ΔE_F), total magnetic moment (M_T), and magnetic moment per atom ($M_{\mu B}$/atom) of (c-g) Ni_{n+1} and (h-l) Ni_nCu clusters (1 ≤ n ≤ 12) with LDA (orange balls) and PBE (blue balls) functionals. The black balls represent the experimental values inserted for comparison (*Phys. Rev. Lett.* 1996, *76*, 1441).

Table A.2: The mixing energy (E_{mix}) per atom and fragmentation energy ($\Delta E_{F(Cu)}$) of Ni_nCu clusters ($1 \leq n \leq 12$) (in lower panel).

Clusters	E_{mix} (eV/atom)	$\Delta E_{F(Cu)}$ (eV)	
	LDA	LDA	GGA
NiCu	0.15	2.92	2.29
Ni_2Cu	0.05	2.60	1.90
Ni_3Cu	0.03	2.89	2.23
Ni_4Cu	0.006	3.58	2.83
Ni_5Cu	0.009	3.73	3.15
Ni_6Cu	-0.001	3.65	2.87
Ni_7Cu	0.01	3.74	2.87
Ni_8Cu	-0.001	3.75	2.98
Ni_9Cu	-0.005	3.57	2.84
$Ni_{10}Cu$	-0.008	3.81	2.75
$Ni_{11}Cu$	-0.0007	3.70	2.86
$Ni_{12}Cu$	-0.003	3.69	3.03

A.5 Theoretical analysis of quantum chemical descriptors.

The spin-dependent quantum chemical descriptors (*J. Phys. Chem. C* **2019**, *123*, 26583-26596) attained with PBE functional such as highest occupied molecular orbital (HOMO)-lowest unoccupied molecular orbital (LUMO) energy gap (E_g), electronegativity (χ), global hardness (η), global softness (S) and an electrophilicity index (ω) for Ni_{n+1} and Ni_nCu clusters obtained with PBE functional are plotted in Figure A.4(a-j) and values obtained with LDA functional are presented in Table A.3 and Table A.4.

$$E_g = E_{LUMO} - E_{HOMO} \qquad (A.8)$$

$$\chi = -\mu = \frac{I + A}{2} \qquad (A.9)$$

$$\eta = E_g = \frac{I - A}{2} \qquad (A.10)$$

$$S = \frac{1}{2\eta} \qquad (A.11)$$

$$\omega = \frac{\mu^2}{2\eta} \qquad (A.12)$$

where μ represents the chemical potential of the system.

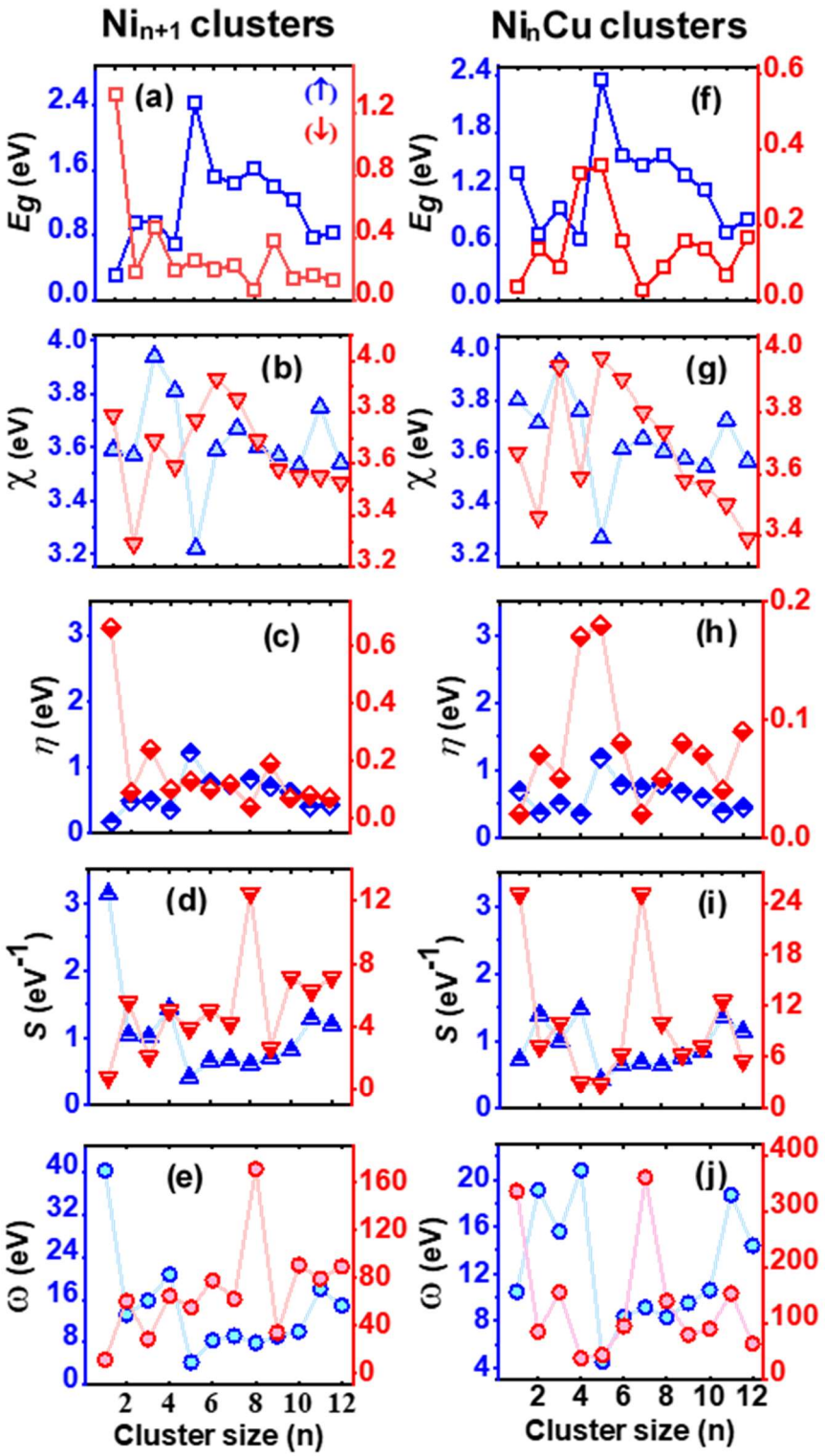

Figure A.4: The highest occupied molecular orbital (HOMO)-lowest unoccupied molecular orbital (LUMO) energy gap (E_g), electronegativity (χ), global hardness (η), global softness (S), and an electrophilicity index (ω) of (a-e) Ni_{n+1} and (f-j) Ni_nCu clusters ($1 \leq n \leq 12$) for spin-up ($\uparrow$) and spin-down ($\downarrow$) states obtained with PBE functionals. The symbols in blue and red color display spin-up ($\uparrow$) and spin-down ($\downarrow$) states, respectively.

Table A.3: The spin-dependent highest occupied molecular orbital (HOMO)-lowest unoccupied molecular orbital (LUMO) energy gap (E_g eV), electronegativity (χ eV), global hardness (η eV), global softness (S eV^{-1}), and an electrophilicity index (ω eV) of Ni_{n+1} clusters ($1 \leq n \leq 12$).

Cluster	LDA (spin-up)					LDA (spin-down)				
	E_g	χ	η	S	ω	E_g	χ	η	S	ω
Ni_2	1.59	4.09	0.80	0.63	10.46	0.06	4.01	0.03	16.67	268
Ni_3	0.94	3.69	0.47	1.06	14.49	0.16	3.48	0.08	6.25	75.69
Ni_4	0.89	3.95	0.45	1.11	17.34	0.39	3.70	0.20	2.50	34.23
Ni_5	0.67	3.97	0.34	1.47	23.18	0.13	3.80	0.07	7.14	103.14
Ni_6	2.55	3.43	1.28	0.39	4.60	0.29	4.32	0.15	3.33	62.21
Ni_7	1.54	3.80	0.77	0.65	9.38	0.07	4.23	0.04	12.50	223.66
Ni_8	1.49	3.90	0.75	0.67	10.14	0.05	4.14	0.03	16.67	285.66
Ni_9	1.60	3.87	0.80	0.63	9.36	0.07	4.13	0.04	12.50	213.21
Ni_{10}	1.41	3.83	0.71	0.70	10.33	0.22	3.92	0.11	4.55	69.85
Ni_{11}	1.23	3.78	0.62	0.81	11.52	0.17	3.93	0.09	5.56	85.81
Ni_{12}	0.73	4.00	0.37	1.35	21.62	0.17	3.97	0.09	5.56	87.56
Ni_{13}	0.88	3.80	0.44	1.14	16.41	0.20	3.80	0.10	5.00	72.20

Table A.4: The spin-dependent highest occupied molecular orbital (HOMO)-lowest unoccupied molecular orbital (LUMO) energy gap (E_g eV), electronegativity (χ eV), global hardness (η eV), global softness (S eV^{-1}), and an electrophilicity index (ω eV) of Ni_nCu clusters ($1 \leq n \leq 12$).

Cluster	LDA (spin-up)					LDA (spin-down)				
	E_g	χ	η	S	ω	E_g	χ	η	S	ω
NiCu	1.5	4.06	0.75	0.67	10.99	0.86	3.74	0.43	1.16	16.26
Ni_2Cu	0.77	3.66	0.39	1.28	17.17	0.08	3.50	0.04	12.50	153.13
Ni_3Cu	0.72	3.71	0.36	1.39	19.12	0.21	3.46	0.11	4.55	54.42
Ni_4Cu	0.66	3.98	0.33	1.52	24.00	0.21	3.81	0.11	4.55	65.98
Ni_5Cu	2.48	3.44	1.24	0.40	4.77	0.19	4.41	0.10	5.00	97.24
Ni_6Cu	1.54	3.83	0.77	0.65	9.53	0.26	4.25	0.13	3.85	69.47
Ni_7Cu	1.47	3.89	0.74	0.68	10.22	0.03	4.21	0.02	25.00	443.10
Ni_8Cu	1.51	3.87	0.76	0.66	9.85	0.07	4.15	0.04	12.50	215.28
Ni_9Cu	1.38	3.85	0.69	0.72	10.74	0.08	3.90	0.04	12.50	190.13
$Ni_{10}Cu$	1.16	3.79	0.58	0.86	12.38	0.15	3.94	0.08	6.25	97.02
$Ni_{11}Cu$	0.70	3.96	0.35	1.43	22.40	0.09	3.90	0.05	10.00	152.10
$Ni_{12}Cu$	0.74	3.78	0.37	1.35	19.31	0.16	3.76	0.08	6.25	88.36

A.6 Adsorption energetics of CO on Ni_{n+1} and Ni_nCu clusters

Table A.5: The adsorption energy (E_{ads}) of CO on different adsorption sites of Ni_{n+1} clusters ($1 \leq n \leq 12$) with various functional schemes. The H, B and T represent hollow, bridge and top sites. The (B - H) indicate the migration of CO from bridge site to hollow site after relaxation. The A and B superscript represent the icosahedral and hcp structure of Ni_{13} cluster, respectively.

Structure	E_{ads} (eV)				
	LDA	LDA-D2	PBE	PBE-D2	PBE-D3
Ni_2-CO					
B	-3.09	-3.11	-2.16	-2.29	-2.27
T	-2.35	-2.38	-1.83	-1.99	-1.97
Ni_3-CO					
B	-2.85	-2.91	-2.19	-2.19	-2.15
T	-2.78	-2.82	-2.23	-2.27	-2.25
Ni_4-CO					
H	-3.09	-3.19	-2.00	-2.08	-2.02
B	-3.02	-3.13	-2.09	-2.18	-2.12
T	-2.92	-3.05	-2.23	-2.30	-2.27
Ni_5-CO					
H	-3.00	-3.16	-2.12	-2.23	-2.16
B	-2.94	-3.08	-2.22	-2.31	-2.26
T	-2.59	-2.65	-2.00	-2.05	-2.04
Ni_6-CO					
H	-2.91	-3.21	-1.90	-2.01	-1.94
B	-2.73	-3.01	-1.86	-1.99	-1.92
T	-2.77	-3.02	-2.09	-2.16	-2.14
Ni_7-CO					
H	-2.69	-3.06	-1.73	-1.86	-1.78
B	-2.69	-3.05	-1.80	-1.90	-1.85
T	-2.35	-2.67	-1.84	-1.89	-1.88
Ni_8-CO					
H	-2.70	-3.19	-1.73	-1.92	-1.77
B	-2.48	-2.96	-1.82	-1.92	-1.85
T	-2.57	-2.63	-1.95	-2.02	-2.00
Ni_9-CO					
H	-2.39	-3.11	-1.46	-1.59	-1.50
B	-2.73 (B – H)	-3.19	-1.67	-1.79	-1.73
T	-2.43	-3.08	-1.92	-1.98	-1.96

Ni_{10}-CO					
H	-2.58	-3.29	-1.67	-1.80	-1.72
B	-2.44	-3.21	-1.68	-1.79	-1.74
T	-2.16	-2.21	-1.69	-1.74	-1.72
Ni_{11}-CO					
H	-2.66	-3.52	-1.77	-1.89	-1.80
B	-2.57	-3.39	-1.88	-1.97	-1.90
T	-2.41	2.49	-1.92	-1.98	-1.95
Ni_{12}-CO					
H	-3.06	-4.09	-2.24	-2.37	-2.31
B	-3.06 (B - H)	-4.09 (B - H)	-2.15	-2.25	-2.21
T	-2.58	-3.60	-2.05	-2.14	-2.11
$^{A}Ni_{13}$-CO					
H	-3.04	-3.22	-2.24	-2.39	-2.31
B	-2.86	-3.03	-2.20	-2.34	-2.27
T	-2.74	-2.89	-2.26	-2.36	-2.33
$^{B}Ni_{13}$-CO					
H	-2.70	-2.86	-1.82	-1.96	-1.88
B	-2.67	-2.80	-1.94	-2.05	-2.00
T	-2.19	-2.27	-1.60	-1.65	-1.63

Table A.6: The adsorption energy (E_{ads}) of CO on different adsorption sites of Ni_nCu clusters ($1 \leq n \leq 12$) with various functional schemes. The H, B and T represent hollow, bridge and top sites. The B - H and H – B indicate the migration of CO from bridge to hollow site and hollow to bridge site respectively after relaxation. The A and B superscript represent the icosahedral and hcp structure of $Ni_{12}Cu$ cluster, respectively.

	E_{ads} (eV)				
Structure	LDA	LDA-D2	PBE	PBE-D2	PBE-D3
NiCu-CO					
T-(Ni)	-2.36	-2.39	-1.98	-2.05	-2.05
T-(Cu)	-1.99	-2.02	-1.44	-1.52	-1.50
Ni_2Cu-CO					
B (Ni-Ni)	-3.19	-3.24	-2.43	-2.44	-2.40
T-(Ni)	-2.97	-3.03	-2.46	-2.46	-2.43
T-(Cu)	-2.39	-2.43	-1.83	-1.87	-1.86
Ni_3Cu-CO					
B (Ni-Ni)	-2.44	-2.55	-1.82	-1.89	-1.86
T-(Ni)	-2.52	-2.60	-1.93	-1.98	-1.96
T-(Cu)	-2.20	-2.30	-1.21	-1.26	-1.25

Ni_4Cu-CO					
B (Ni-Ni)	-2.78	-2.89	-1.98	-1.97	-2.03
T-(Ni)	-2.97	-3.02	-2.22	-2.37	-2.27
T-(Cu)	-1.73	-1.78	-1.25	-1.30	-1.29
Ni_5CuCO					
B (Ni-Ni)	-2.72	-2.85	-1.76	-1.87	-1.81
T-(Ni)	-2.76	-2.85	-2.01	-2.11	-2.08
T-(Cu)	-2.03	-2.11	-1.41	-1.48	-1.47
Ni_6Cu-CO					
B (Ni-Ni)	-2.49	-2.62	-1.85	-1.67	-1.91
T-(Ni)	-2.83	-2.95	-2.09	-2.19	-2.16
T-(Cu)	-1.77	-1.82	-1.23	-1.28	-1.27
Ni_7Cu-CO					
B (Ni-Ni)	-2.54	-2.69	-1.82	-1.75	-1.87
T-(Ni)	-2.62	-2.75	-1.85	-1.97	-1.92
T-(Cu)	-1.80	-1.86	-1.30	-1.35	-1.34
Ni_8Cu-CO					
B (Ni-Ni)	-2.17	-2.33	-1.52	-1.64	-1.52
T-(Ni)	-2.44	-2.59	-1.78	-1.87	-1.86
T-(Cu)	-1.66	-1.76	-1.17	-1.22	-1.21
Ni_9Cu-CO					
B (Ni-Ni)	-2.20	-2.35	-1.40	-1.56	-1.49
T-(Ni)	-2.30	-2.42	-1.80	-1.92	-1.87
T-(Cu)	-1.62	-1.67	-1.16	-1.20	-1.19
$Ni_{10}Cu$-CO					
B (Ni-Ni)	-2.29	-2.43	-1.65	-1.82	-1.72
T-(Ni)	-2.41	-2.49	-1.90	-1.94	-1.94
T-(Cu)	-1.76	-1.81	-1.28	-1.34	-1.33
$Ni_{11}Cu$-CO					
H - B	-2.90	-3.01	-2.18	-2.30	-2.25
B (Ni-Ni)	-1.78	-1.86	-2.08	-2.19	-2.16
T-(Ni)	-2.62	-2.00	-2.08	-2.18	-2.15
$^{A}Ni_{12}Cu$-CO					
B (Ni-Ni)	-2.91	-3.07	-2.20	-2.35	-2.27
T-(Ni)	-2.80	-2.93	-2.28	-2.38	-2.35
T-(Cu)	-1.89	-2.00	-1.39	-1.48	-1.45
$^{B}Ni_{12}Cu$-CO					
B - H	-2.33	-2.48	-1.59	-1.87	-1.68
T-(Cu)	-1.55	-1.60	-1.06	-1.10	-1.09